JOURNAL OF Materials CHEMISTRY

The optical gas-sensing properties of an asymmetrically substituted porphyrin

José Mª Pedrosa,*[a] Colin M. Dooling,[b] Tim H. Richardson,[b] Robert K. Hyde,[c] Chris A. Hunter,[c] Mª Teresa Martín[a] and Luis Camacho[a]

[a]*Departamento de Química Física y Termodinámica Aplicada, Universidad de Córdoba, Campus Universitario de Rabanales, E-14014, Córdoba, Spain. E-mail: qf2pepoj@uco.es; Fax: +34 957 21 88 42; Tel: +34 957 21 86 47*
[b]*Department of Physics & Astronomy, University of Sheffield, Hounsfield Road, Sheffield, UK S3 7RH*
[c]*Department of Chemistry, University of Sheffield, Brook Hill, Sheffield, UK S3 7HF*

Received 22nd May 2002, Accepted 7th June 2002
First published as an Advance Article on the web 25th July 2002

In this paper we have investigated the NO_2 gas-sensing properties of LB film assemblies of 5,15-bis(4-aminophenyl)-10,20-bis[3,4-bis(2-ethylhexyloxy)phenyl]-21*H*,23*H*-porphine (CAH4). The optical absorbance spectrum of these films is dramatically affected when exposed to low concentrations of NO_2 gas. LB films of CAH4 were prepared by using ultra-fast deposition and characterized by imaging ellipsometry. The high deposition rates employed (500 mm min^{-1}) led to an inhomogeneous structure with high porosity. The LB film exposed to 4.6 ppm NO_2 showed a sensitivity of 60% relative absorbance change at 439 nm. The response was found to be faster than that measured in similar systems. The fast response can be explained in terms of the molecular structure of the porphyrin as well as the enhanced surface area of the porous film. The optical response of the CAH4 film gradually decreases as its temperature is increased, a result of a shift in the adsorption–desorption equilibrium towards desorption. An activation energy of 0.48 eV is obtained. Full recovery of the original spectrum after exposure to NO_2 is obtained and can be dramatically accelerated with gentle heating (353 K). The concentration dependence of the optical response over the range 0.46–4.6 ppm NO_2 obeyed a Langmuir adsorption model. Ageing experiments have shown that the basic response of the CAH4 assemblies is not affected over a time period of at least 1 year.

Introduction

Stricter controls on the emission of toxic gases into the environment have increased the need for cheaper, sensitive and reversible gas sensors.[1,2] Pollutants such as NO_2, SO_2 or Cl_2 require monitoring at concentrations as low as a few parts per million (ppm). At present the most commonly used commercial sensor devices are based on semiconducting inorganic oxides.[3] These devices generally use the transport of electrons through the sensor layer in the presence of the analyte gas. However, most available devices present disadvantages such as the high operating temperatures required (400–600 °C) or low output signal level.

Several researchers have suggested using organic materials deposited as thin films as active elements in gas sensors[4–7] to improve the device performance. In this way, phthalocyanines have attracted great interest as organic semi-conductometric sensors.[8,9] However, recent developments based on spectral changes in the optical properties of the organic materials have shown a number of advantages in terms of selectivity, sensitivity and response time.[10,11] In particular, porphyrin thin films have shown promise as useful optical gas-sensing materials.[12,13*a*] A successful sensor must be capable of providing an easily measurable signal in response to the interaction of the sensing agent with the ion or molecule to be detected. Porphyrins are highly conjugated organic molecules that possess high chemical stability and favourable optical properties including gas-sensitive visible absorption spectra and are compatible with the use of cheap light emitting diodes in commercial devices.

In preliminary studies,[13*b*] monolayers of 5,15-bis(4-aminophenyl)-10,20-bis[3,4-bis(2-ethylhexyloxy)phenyl]-21*H*,23*H*-porphine (CAH4) have been characterized at the air–water interface by Brewster angle microscopy (BAM) and reflection spectroscopy. The results showed that CAH4 spontaneously formed domains of self-aggregated molecules before compression of the Langmuir film. The reduction of the area per molecule resulted in a higher degree of aggregation, which basically was maintained during the LB transfer process. LB films of CAH4 prepared by the ultra-fast deposition method were exposed to low concentrations of NO_2 and the influence of the molecular packing on the gas response was investigated. Repeated exposures did not result in a loss of response, suggesting CAH4 as a promising gas-sensing material. Here, we present a detailed study of the NO_2 optical sensing properties of CAH4 assemblies. This study includes gas concentration and temperature dependence investigations as well as the effect of ageing. Also, two possible sensing mechanisms for the gas–porphyrin interaction will be discussed.

Experimental

Materials

UV-visible spectra of CAH4 in chloroform solution were recorded on a Cary 100 Bio UV-visible spectrophotometer using quartz cuvettes. The absorbance of the Soret band (427 nm) as a function of CAH4 concentration was found to be linear in the concentration range 2×10^{-6}–2×10^{-4} M. Mass spectra were obtained on a Fisons/VG Pro Spec 3000 using a *m*-nitrobenzyl alcohol matrix. Column chromatography was carried out using Florisil 100–200 mesh (Aldrich) and silica gel (40–63 μm). Nuclear magnetic resonance (NMR) spectroscopy was performed on a Bruker AM-250 MHz, operating as a Fourier transform machine. All spectra were referenced to $CHCl_3$. Melting

points were performed on a Reichter Kofler hot stage melting point apparatus.

Dichloromethane was supplied by Fisher and was stabilised with amylene (0.02%). It was purified and dried by distillation over calcium hydride. Dry ethanol was obtained by distillation over molecular sieves (4 Å) and stored over molecular sieves (4 Å). Triethylamine was dried by storage over 4 Å molecular sieves.

3,4 Dihydroxybenzaldehyde and 2-ethylhexyl bromide were supplied by Lancaster. Aldrich supplied all other reagents. All reagents were used as received except pyrrole, which was distilled fresh on the day of use.

Synthesis of CAH4

The synthesis and structure of 5,15-bis(4-aminophenyl)-10,20-bis[3,4-bis(2-ethylhexyloxy)phenyl]-21*H*,23*H*-porphine (CAH4) is shown in Scheme 1 and described below.

5,15-Bis(4-nitrophenyl)-10,20-bis[3,4-bis(2-ethylhexyloxy)-phenyl]-21*H*,23*H*-porphine. In a light-protected flask a solution of 3,4-bis(2-ethylhexyloxy)benzaldehyde (synthesis described elsewhere[13a]) (90.5 mg, 0.25 mmol) and *meso*-(4-nitrophenyl)-dipyrromethane (synthesis described elsewhere[14]) (66.8 mg, 0.25 mmol) in $CHCl_3$ (25 cm^3) was purged with N_2 for 10 minutes, then boron trifluoride–diethyl ether (33 μl of 2.5 M stock solution in $CHCl_3$, 83 μmol) was added. The solution was stirred under N_2 for 1 hour at room temperature. 2,3-Dichloro-5,6-dicyano-1,4-benzoquinone (43 mg, 0.19 mmol) was added and the mixture stirred for another hour. The solvent was removed with a rotary evaporator. The residue was dissolved in a small amount of CH_2Cl_2, and purified by column chromatography, eluting with CH_2Cl_2–petroleum ether. The first coloured band to be eluted contained the required product. Further purification by column chromatography was necessary to obtain pure 5,15-bis(4-nitrophenyl)-10,20-bis[3,4-bis(2-ethylhexyloxy)phenyl]-21*H*,23*H*-porphine which was recrystallised from $CHCl_3$–MeOH to give a purple powder with a yield of 51.6 mg (4.0 μmol, 33%).

^{1}H NMR (250 MHz, $CDCl_3$): δ (ppm) = 8.96 (d, J = 4.9 Hz, 4 H), 8.78 (d, J = 4.9 Hz, 4 H), 8.62 (d, J = 8.85 Hz, 4 H), 7.75 (d, J = 8.85 Hz, 4 H), 7.75 (s, 2 H), 7.69 (dd, J = 2.1 and 8.2 Hz, 2 H), 7.24 (d, J = 8.2 Hz, 2 H), 4.12 (d, J = 5.8 Hz, 4 H), 4.03 (d, J = 6.1 Hz, 4 H), 0.82 – 1.92 (m, 60 H), −2.75 (s, 2 H). ^{13}C NMR (62.9 MHz, $CDCl_3$): δ (ppm) = 149.6 (C), 149.0 (C), 147.7 (C), 147.5 (C), 135.0 (CH), 133.9 (C), 127.6 (CH), 121.8 (CH), 121.2 (C), 120.6 (CH), 117.3 (C), 116.8 (C), 111.5 (CH), 71.9 (CH_2), 71.7 (CH_2), 39.8 (CH), 39.7 (CH), 30.7 (CH_2), 30.6 (CH_2), 29.3 (CH_2), 29.1 (CH_2), 24.1 (CH_2), 23.9 (CH_2), 23.1 (CH_2), 23.0 (CH_2), 14.1 (CH_3), 14.0 (CH_3), 11.3 (CH_3), 11.2 (CH_3). MS (TOF MS ES+): m/z (%) = 1220 [M − H + 2]$^+$ (15), 1219 [M − H + 1]$^+$ (69), 1218 [M − H]$^+$ (100). HR-MS ($C_{76}H_{93}N_6O_8$): calc. 1157.7517; found 1157.7517. UV-VIS ($CHCl_3$): λ_{max}/nm (ε × 10^{-3} l mol^{-1} cm^{-1}) = 427.0 (227), 519.7 (16), 557.8 (11), 593.6 (6), 651.2 (5). Melting point: 166–167 °C.

5,15-Bis(4-aminophenyl)-10,20-bis[3,4-bis(2-ethylhexyloxy)-phenyl]-21*H*,23*H*-porphine. In a light-protected flask, 5,15-bis-(4-nitrophenyl)-10,20-bis[3,4-bis(2-ethylhexyloxy)phenyl]-21*H*,23*H*-porphine (500 mg, 411 μmol) was dissolved in EtOH–EtOAc (1 : 3, 50 cm^3). Stannous chloride (1.85 g, 8.22 mmol) was added and the mixture stirred at 70 °C under N_2. The formation of the product was monitored by TLC, which indicated that a baseline product formed at an equal rate. After 1 hour, the starting material had disappeared. The mixture was allowed to cool, poured onto ice–water (50 cm^3) and extracted with EtOAc (100 cm^3) after basifying with sodium bicarbonate, then dried over anhydrous sodium sulfate. The mixture was filtered, and the solvent was removed with a rotary evaporator. The residue was dissolved in a small amount of CH_2Cl_2 and purified by column chromatography, eluting with CH_2Cl_2–petroleum ether and then MeOH–CH_2Cl_2. 5,15-Bis(4-aminophenyl)-10,20-bis[3,4-bis(2-ethylhexyloxy)phenyl]-21*H*,23*H*-porphine was recrystallised from $CHCl_3$–MeOH to give a purple powder with a yield of 238 mg (206 μmol, 50%).

^{1}H NMR (250 MHz, $CDCl_3$): δ (ppm) = 8.92 (s, 8 H), 7.98 (d, J = 7.6 Hz, 4 H), 7.78 (s, 2 H), 7.70 (d, J = 7.9 Hz, 2 H), 7.23 (d, J = 8.2 Hz, 2 H), 7.04 (d, J = 7.6 Hz, 4 H), 4.16 (d, J = 5.5 Hz, 4 H), 4.03 (d, J = 5.8 Hz, 4 H), 0.81–1.94 (m, 60 H), −2.74 (s, 2 H). ^{13}C NMR (62.9 MHz, $CDCl_3$): δ (ppm) = 149.2 (C), 147.4 (C), 145.9 (C), 135.5 (CH) 134.8 (C), 132.5 (C), 127.5 (CH), 120.6 (CH), 120.2 (C), 119.8 (C), 113.4 (CH), 111.5 (C), 71.9 (CH_2), 71.7 (CH_2), 39.8 (CH), 39.6 (CH), 30.7 (CH_2), 30.6 (CH_2), 29.3 (CH_2), 29.1 (CH_2), 24.1 (CH_2), 23.9 (CH_2), 23.1 (CH_2), 23.0 (CH_2), 14.1 (CH_3), 14.0 (CH_3), 11.3 (CH_3), 11.2 (CH_3). MS (TOF MS ES+): m/z (%) = 1159 [M − H + 1]$^+$ (62), 1158 [M − H]$^+$ (100), 821 (28). HR-MS ($C_{76}H_{97}N_6O_4$): calc. 1217.7055; found 1217.7032. UV-VIS ($CHCl_3$): λ_{max}/nm (ε × 10^{-3} l mol^{-1} cm^{-1}) = 427.3 (328), 521.6 (14), 560.8 (11), 596.0 (5), 653.8 (5). Melting point: 146–147 °C.

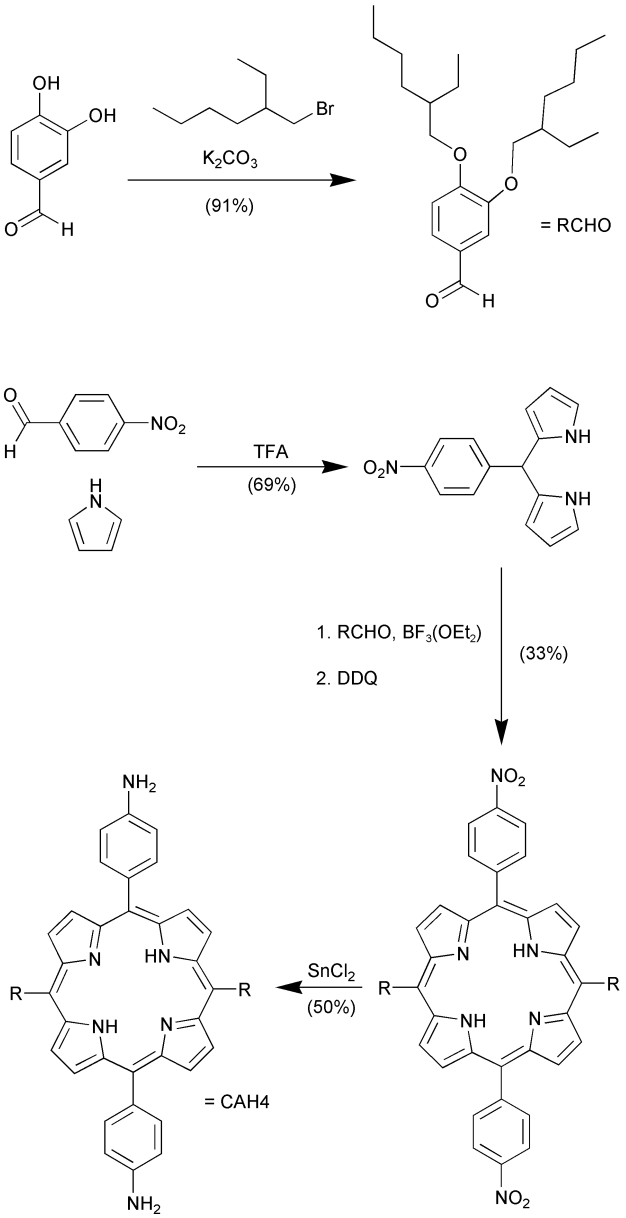

Scheme 1 Synthetic route and structure of CAH4.

Film fabrication and characterization

Monolayers of CAH4 were prepared by spreading a chloroform solution (2×10^{-4} M) onto a clean water surface (pH $\sim$ 6.2, 20 °C) on a constant perimeter Joyce–Loebl minitrough provided with a filter paper Wilhemy plate.[15] After evaporation of the organic solvent, the floating Langmuir film was compressed at a rate of 0.1 nm^2 molecule^{-1} min^{-1} to 19 mN m^{-1} and transferred onto glass plates (rendered hydrophobic by immersion in 1,1,1,3,3,3-hexamethyldisilazane for 24 h) at a rate of 500 mm min^{-1}. Although not successful for all materials, this unconventional high transfer rate was found to be compatible with CAH4. Notes on ultra-fast LB deposition have been published elsewhere.[13a]

The imaging ellipsometry was carried out at room temperature in air using an I-Elli2000 (Nanofilm Technology, Germany) imaging ellipsometer, where light from a 532 nm laser is reflected off the sample and collected using an objective lens and CCD camera. The ellipsometer optics are arranged in a polarizer, compensator, sample, analyzer geometry, and operated at ellipsometric contrast.

Gas testing

A purpose-built gas-testing chamber was used to assess the gas-sensitive optical properties of CAH4 assemblies. This consisted of a gas inlet and outlet, a Peltier heating–cooling stage and housings for fibre optics cables supplying the probe light beam from the tungsten white light source and delivering the light transmitted through the sample to the optical detector. The gas delivery system incorporates two computer-controlled Tylan FC-260 mass flow controllers for defining the relative flows of NO_2 (obtained at 4.6 ppm in dry nitrogen, BOC, UK) and dry N_2 (as a further diluent). This delivery system facilitated the accurate production of dilute toxic gas in the concentration range 0.1–4.6 ppm. The gas mixture was directed into the gas testing chamber that held the CAH4 samples between the two optical fibres. A World Precision Instruments Spectromate spectrophotometer incorporating a multi-channel photodiode array detector was used to record visible absorption spectra over the wavelength range 350–850 nm. Data were collected every 3 s during the gas exposure/recovery cycles. The instrument also displayed changes in the optical absorbance (at preset wavelengths) as a function of time, allowing convenient observation of the kinetics of the sensing process in real time. The exposure occurred at 293 K (unless otherwise stated) and the recovery phase (dry nitrogen only) at 350 K. Long-term ageing experiments involved storing an unexposed film in the dark under ambient conditions for 2 months and 1 year time periods and then comparing its response and recovery characteristics to a freshly prepared film.

Results and discussion

Monolayers of CAH4 were spread on pure water and transferred to hydrophobic glass substrates by ultra-fast LB deposition. The deposition surface pressure was 19 mN m^{-1}, since higher surface pressures caused slow collapse of the layer, while for $\pi < 16$ mN m^{-1} no fast deposition was possible. In previous work,[13a] it has been extensively shown that ultra-fast deposition rates of porphyrin monolayers lead to inhomogeneous (on a micron scale) perforated film structures. This unusual morphology has proved to be very useful in gas sensing, mainly due to the enhanced surface area of the porous film assembly. Fig. 1 is a 3-D plot of an imaging ellipsometer image of a 3-excursion CAH4 film deposited at a rate of 500 mm min^{-1} onto an optically flat hydrophobic glass substrate. One excursion means two passages of the substrate through the floating monolayer, one downwards followed by its subsequent withdrawal. The *Z*-axis only represents the film

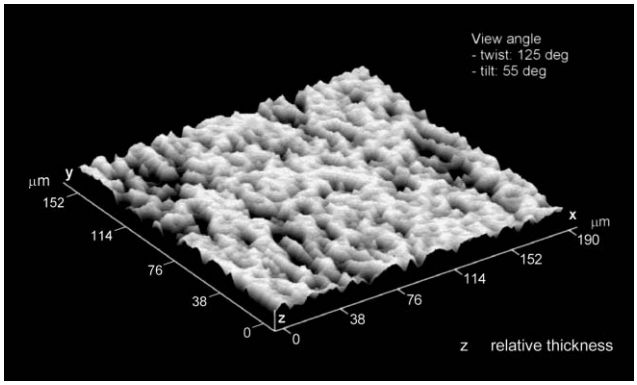

Fig. 1 Imaging ellipsometer image of a 3-excursion CAH4 LB film deposited at 500 mm min^{-1}.

thickness qualitatively. The image shows a morphology characterized by a disordered array of interconnecting porphyrin domains distributed over the surface. This perforated film structure is similar to that observed by atomic force microscopy in LB film assemblies of analogous porphyrins,[13a] which were prepared using the same deposition method.

Thin film gas sensing primarily involves gas adsorption on the film surface. Therefore a porous structure that enhances the surface area and promotes diffusion of the analyte gas through the film improves the sensor behaviour. The mechanism for the formation of the porphyrin domains is still unclear. Images of the bare glass substrate did not show enough surface roughness to explain such topology. Another possible interpretation relies on the island-type morphology existing within the floating film on the water surface itself. However, the CAH4 molecules form a homogeneous and dense film on water at the deposition surface pressure (BAM images not shown here). Finally, a dewetting process of the substrate film during the fast upward transition from the water surface has been pointed out as a possible mechanism.[13a]

Fig. 2 shows the typical response for a 3-excursion CAH4 assembly when exposed to NO_2 gas (4.6 ppm in this experiment). The temporal evolution of the UV-visible absorbance spectrum involves a fast decay of the Soret band (439 nm) intensity coupled to the growth of a new strong band at 472 nm and a weak band at 710 nm. The initial spectrum of the LB film before gas exposure is red shifted by $\sim$13 nm with respect to the solution. This red shift has been attributed to the J-aggregation state of the CAH4 molecules in the solid film. Such aggregation is already present at the air–water interface and is maintained during the transfer process. In any case the spectral changes on exposure to NO_2 are similar to that observed in chloroform solution (data not shown), where the porphyrin molecules are in their monomeric form. Therefore, the aggregation state of the CAH4 molecules in the LB film

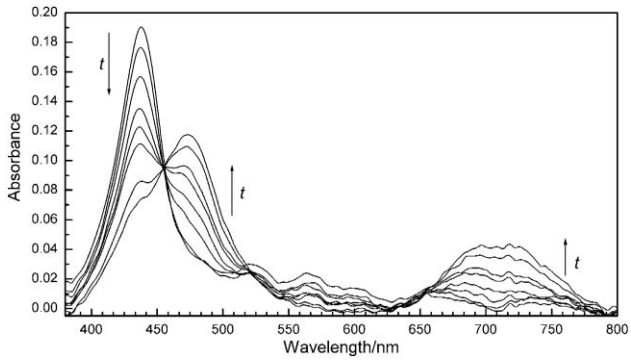

Fig. 2 Temporal evolution of the UV-visible spectrum of an LB film (3-excursion) of CAH4 during exposure to 4.6 ppm NO_2 gas (time interval is 3 s).

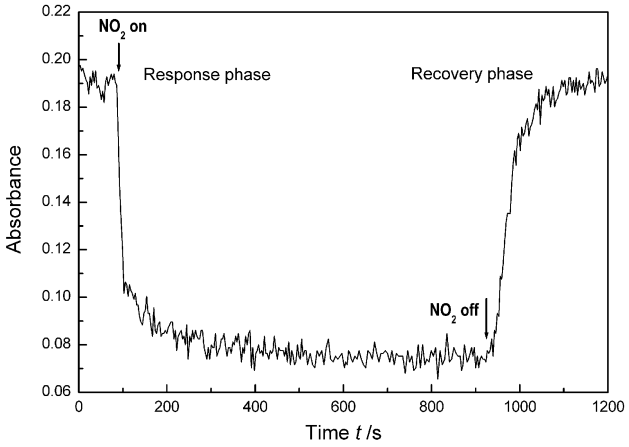

Fig. 3 Absorbance of the Soret band (439 nm) of an LB film of CAH4 (3-excursions) as a function of time during exposure to 4.6 ppm NO_2.

does not have a negative influence on their interaction with the gas molecules.

The evolution of the Soret band (439 nm) intensity as a function of time is shown in Fig. 3. As can be seen, the kinetics of the gas exposure (4.6 ppm NO_2, 293 K) is characterised by a fast decay of the Soret band intensity followed by a slow reduction of this intensity until a saturation value, 60% lower than the original level, is reached. As the NO_2 gas stream is switched off, a dry nitrogen flush is activated whilst the sample is quickly heated to 353 K. This rapidly initiates recovery and after a few seconds the original Soret band intensity has been restored. Repeated cycles of gas exposure and recovery do not result in any loss of response. In order to investigate the possible adsorption processes involved in the response of the CAH4 assemblies to the gas molecules, the Elovich kinetics model[16] was applied. According to this model, the surface coverage, Θ, by the adsorbate gas as a function of time, t, is given by

$$\Theta = \left(\frac{1}{\beta}\right) \ln(t) + K \quad (1)$$

where β and K are constants. This expression is obtained assuming an exponential decrease in the rate of surface coverage as the coverage itself is increased. That is, the probability of adsorption of a gas molecule decreases exponentially as a function of the number of NO_2 molecules already adsorbed. Fig. 4 shows the plot of Θ *versus* ln (t). The relationship is only linear over the first 30 s of the exposure, deviating from linearity at higher time values. This behaviour

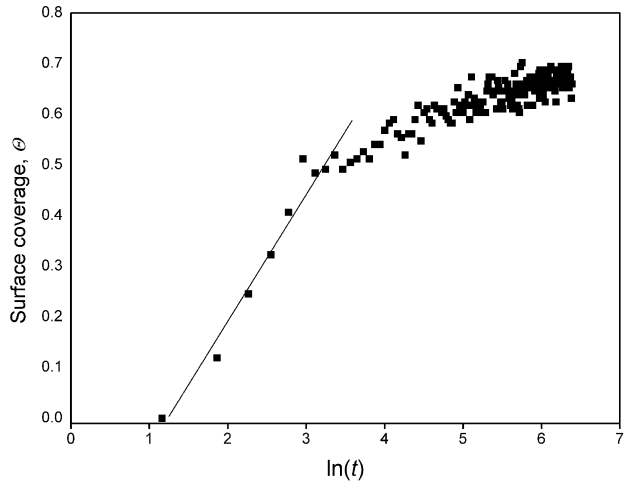

Fig. 4 Elovich response kinetics for a 3-excursion CAH4 LB film (4.6 ppm NO_2).

has been observed in many other thin film organic sensing materials,[13a,17] and the linear region represents a fast surface adsorption process whilst the deviation from linearity results from slow diffusion of the gas molecules into the buried layers of the film. Another possible interpretation for such deviation from linearity arises from the presence of several different types of adsorption sites in the irregular film structure. In any case, for the CAH4 assemblies the linear region involves the major part of the total absorbance change, resulting in an initial adsorption process that is surprisingly fast. To characterize the speed of response and recovery the parameters t_{50} and t_{90} can be used. These are defined as the time taken for the Soret band intensity to reach the 50% and 90% of its final saturated value respectively. Table 1 indicates these values for both the response and the recovery phases. They all reflect that the CAH4 assemblies behave as fast sensors. In particular, t_{50} for the response phase has been found to be at least half those measured for similar porphyrin assemblies[13a] and considerably smaller than those values typically reported for different molecular systems like phthalocyanines. It should be pointed out that conventional deposition rates (10 mm min^{-1}) or other deposition methods, such as solution casting, did not improve the NO_2 gas-sensing characteristics of the porphyrin under study, showing slower rates of response and recovery. Therefore, the faster temporal response of the CAH4 LB films prepared by ultra-fast deposition can be attributed (at least in part) to the higher surface area to volume ratio of these assemblies.

There are two possible mechanisms for the NO_2–porphyrin reaction. One of them involves protonation of the porphyrin ring to form the porphyrin dication. In this process, NO_2 molecules must dissolve in water to produce nitrous and nitric acid that attack the porphyrin core. It should be noted that dry gases were used in all the experiments; therefore, moisture within the film would be required to facilitate protonation. It is well known that in most cases, acidification of porphyrin organic solutions yields similar spectral changes to those observed for the CAH4–NO_2 gas system (Fig. 2). However, full recovery of the LB film would imply a further chemical reaction with other species, like alkalis, to restore the porphyrin to its unprotonated form. CAH4 assemblies show full recovery of the original spectrum by simply flushing with dry nitrogen and gentle heating (350 K). In principle, these conditions would be insufficient for the recovery of the protonated porphyrin.

An alternative mechanism, previously proposed for similar systems,[18] involves the interaction of the electrophilic NO_2 gas with the active porphyrin sites. Thus, a charge-transfer type bond between the incoming NO_2 and the same sites where protonation occurs would account for similar spectral changes. Moreover, the presence of the electron-donating aminophenyl groups in the *meso* positions of the porphyrin ring would increase the charge-transfer interaction improving the gas-sensing characteristics of the CAH4 assemblies. Finally, full recovery can easily occur with the application of heat because of the lower binding energy of the charge-transfer bond as compared to the covalent bonds involved in the protonation of the porphyrin molecules.

Table 1 The t_{50} and t_{90} values for 3-excursion CAH4 LB films fresh and aged (2 months and 1 year). The relative Soret band absorbance change is also shown for the three films

	Speed of response and recovery				
	Response phase		Recovery phase		Relative absorbance change (%)
Time after deposition	t_{50}/s	t_{90}/s	t_{50}/s	t_{90}/s	
2 days	10	44	35	92	60
2 months	11	50	32	70	58
1 year	10	90	39	74	58

At this point, it should be added that the influence of other normal components of air, such as water vapor or oxygen, was not tested given that only dry nitrogen was used as diluent. It is assumed that moisture is present within the freshly prepared CAH4 assemblies, and no differences in the NO_2 gas-sensing properties were observed between these films and those stored in a dry atmosphere (data not shown). Therefore, the interference of water, *via* an hydrolysis/protonation mechanism, appears to be little plausible. However, oxygen is a competing electron acceptor and the need to displace these molecules, bound by weak charge-transfer interactions, from the donor surface, could slow down the response kinetics of the CAH4 gas-sensing devices. Further experiments concerning the use of normal air as diluent are a subject of future work.

The effect of the NO_2 concentration on the response of CAH4 assemblies was also investigated. Reversible and reproducible exposure–recovery cycles were obtained over the NO_2 concentration range 0.46–4.6 ppm, as shown in Fig. 5. In all the exposures the temperature was maintained at 293 K while the recovery was performed at 353 K. It is clear that the response increases with increasing gas concentration. In order to quantify the concentration dependence of the response, a number of isotherm models, which describe the adsorption/desorption of the gas molecules onto the solid surface, can be applied.[19] One of them is the Langmuir adsorption isotherm,[20] and even though this model is one of the simplest to describe the adsorption of a gas onto a solid surface, it has been used by a number of workers to characterise their systems,[18,21] and provides a preliminary insight into the active adsorption process. The Langmuir adsorption isotherm is usually expressed by

$$\frac{n_{ads}}{N_s} = \frac{\lambda c}{1+\lambda c} \tag{2}$$

where n_{ads} is the number of gas molecules adsorbed (which is proportional to the change in Soret band absorbance, ΔAbsorbance), N_s is the number of adsorption sites, λ is a constant relating to the adsorbability of the gas and c is the concentration of the gas, $[NO_2]$.

Rearrangement of eqn. (2) leads to

$$\left(\frac{c}{n_{ads}}\right) = \left(\frac{c}{N_s}\right) + \left(\frac{1}{N_s\lambda}\right) \tag{3}$$

This expression is known as the linear form of the Langmuir adsorption isotherm; thus a plot of c/n_{ads} *versus* c should yield a straight line if the assumptions on which it is based are valid. These assumptions are that the activation energy for adsorption is the same for all binding sites in the thin film assembly, that there are a fixed number of localised surface sites present on the surface and that NO_2 molecules striking a surface site that is already occupied do not adsorb. This latter assumption limits the adsorption of NO_2 onto a thin organic film surface to a single monolayer. Fig. 6 shows a plot of c/Δabsorbance *vs.* c, and a straight line is obtained, indicating that Langmuir adsorption, even with its limited assumptions, provides a basic understanding of the NO_2–CAH4 interaction during the sensing process.

The temperature dependence of the gas response is also an important characteristic to be studied in a gas sensor, since it can help to set the optimum operating conditions. Fig. 7 depicts a sequence of gas exposure–recovery cycles in which the gas exposure is performed over the temperature range 293–348 K. In all cases the recovery phase was performed at 353 K. As can be seen, the magnitude of the gas response falls off rapidly as the temperature increases. This behaviour can be explained in terms of a shift towards desorption of the adsorption–desorption dynamic equilibrium of the NO_2 molecules as the temperature is increased. The relationship between the optical absorbance change of the Soret band and the temperature can be used to evaluate the activation energy, ΔE_{ads}, for the NO_2–CAH4 adsorption process. Fig. 8 shows an Arrhenius plot for the gas response of a CAH4 LB film (3-excursions) when exposed to 4.6 ppm NO_2. The gradient of this plot yields $\Delta E_{ads}/k$ (where k is Boltzmann's constant) leading to a value for ΔE_{ads} of 0.48 eV. ΔE_{ads} values below 0.2 eV can be related to easy adsorption/desorption processes but also to very low sensitivity. On the other hand, activation energies above 1 eV are indicative of high sensitivity but extremely long recovery times at room temperature. Therefore, the value of 0.48 eV represents an intermediate situation

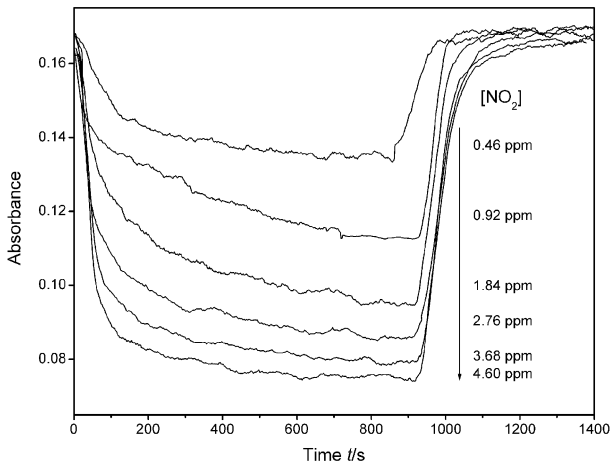

Fig. 5 Effect of the NO_2 concentration on the absorbance change at 439 nm of a 3-excursion CAH4 LB film.

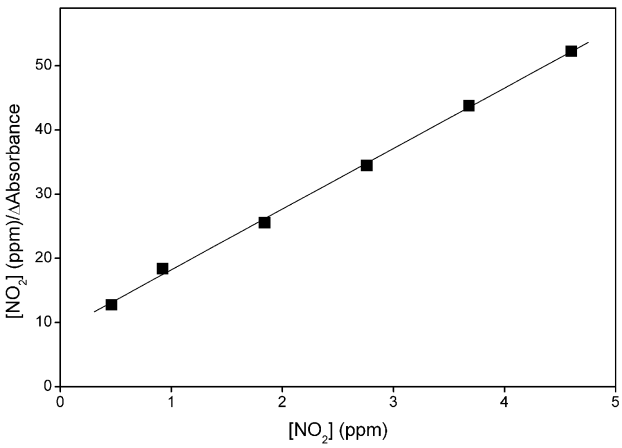

Fig. 6 Langmuir adsorption plot for a 3-excursion CAH4 LB film.

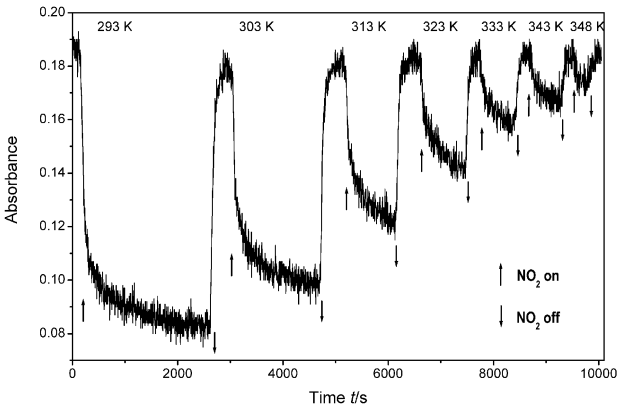

Fig. 7 A sequence of exposure cycles (4.6 ppm NO_2) performed over the temperature range 293–348 K. The temperature for the recovery phase is 353 K in all cases.

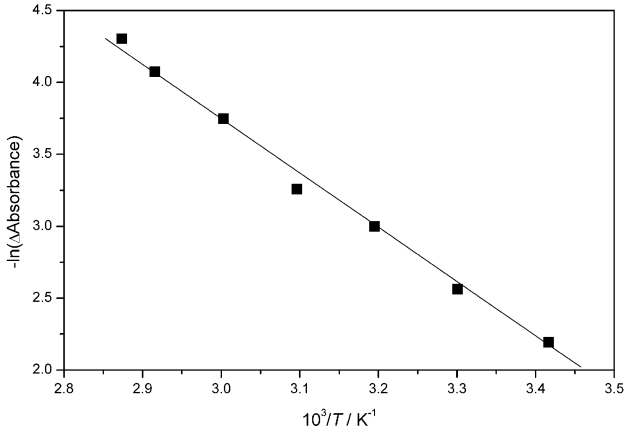

Fig. 8 Arrhenius plot for a 3-excursion CAH4 LB film exposed to 4.6 ppm NO_2.

leading to moderate sensitivity and recovery rates. Temperature dependence experiments of the recovery kinetics over the range 323–353 K were also made and the results, not shown here, showed that the rate of recovery is accelerated as the sample temperature increases. This is also explained in terms of shifts in the adsorption–desorption equilibrium.

Although theoretically the simple adsorption models underlying the linear relationships in Figs. 4, 6 and 8 are not expected to be strictly valid for heterogeneous films such as those used here, it is clear from our data that the empirical linear fits are useful for predicting the gas-sensing behaviour as a function of concentration and temperature. In particular the CAH4 film assemblies are able to detect very low concentrations (up to 0.46 ppm) of NO_2 gas, operating between 293 K and 353 K for the exposure and recovery cycles respectively. However, some improvements such as a lower detection limit or higher operation temperatures are needed to ensure the applicability of the proposed system. Future work will be directed towards this.

Finally, the effect of long-term storage under normal air atmosphere at room temperature in the dark on the gas response and recovery was investigated. Table 1 shows the t_{50} and t_{90} for the response and recovery phases as well as the relative absorbance change of the response for freshly prepared and aged (2 months and 1 year respectively) samples. It can be seen that the t_{50} remains nearly unaltered for both the response and the recovery phases in all the samples, irrespective of the storage time. For the t_{90}, however, some differences are detected. In this latter case, the ageing results in an increment of the response time and a reduction of the recovery time. As has been discussed above, the t_{50} refers to a fast surface adsorption process of the gas molecules, while the t_{90} relates to a slow gas diffusion process into the film structure. Therefore, the differences observed for the t_{90} times can be explained on the basis of small changes in the internal structure of the film, which can alter the adsorption–desorption equilibrium in the diffusion process. In any case, the magnitude of the response does not change and hence the sensitivity of the sensor remains unaltered.

Conclusions

LB film assemblies of CAH4 prepared by ultra-fast deposition have been shown to exhibit a fast response (t_{50} = 10 s) when exposed to 4.6 ppm of NO_2. At this gas concentration, a relative absorbance change of around 60% was measured. The morphology of these LB assemblies was studied using imaging ellipsometry; the images show a disordered array of porphyrin domains that lead to an inhomogeneous perforated film. The fast response to NO_2 can be explained in terms of the enhanced surface area of this structure as well as the molecular functionality of the porphyrin. Concentration and temperature dependence experiments show that CAH4 LB assemblies are particularly useful for very low NO_2 concentrations (0.46–4.6 ppm) operating at room temperature. Full fast recovery can be achieved with gentle heating (353 K). Ageing experiments have shown that the basic response of the film is not affected over a time period of at least 1 year. In order to assess the selectivity of the CAH4 LB films, preliminary results on their response to other toxic gases such as Cl_2 and HCl have been obtained. Although the CAH4 assemblies also respond to these gases, a marked difference in its response was observed, suggesting that the spectral profile of the exposed films may facilitate gas identification as well as its concentration measurement. This will be detailed in a future publication.

Acknowledgements

The authors wish to express their gratitude to the Spanish DGICyT for financial support (Project PB97-0453). We also would like to thank Dr D. Hönig (NFT, Germany) for the imaging ellipsometer measurements.

References

1 A. Mandelis and C. Christofides, *Solid State Gas Sensor Devices*, **Vol. 125** in the *Chemical Analysis Series*, Wiley, New York, 1993.
2 J. Madou and S. R. Morrison, *Chemical Sensing with Solid State Devices*, Academic Press, New York, 1989.
3 P. T. Moseley, J. O. W. Norris and D. E. Williams, *Techniques and mechanisms in gas sensing*, Adam Hilger, Bristol, 1991.
4 J. Kaufhold and K. Hauffe, *Ber. Bunsen-Ges. Phys. Chem.*, 1965, **69**, 168.
5 M. A. Arnold, *Anal. Chem.*, 1992, **64**, 1015A.
6 M. C. Lonergan, E. J. Severin, B. J. Doleman, S. A. Beaber, R. H. Grubb and N. S. Lewis, *Chem. Mater.*, 1996, **8**(9), 2298.
7 A. K. Hassan, A. K. Ray, J. R. Travis, Z. Ghassemlooy, M. J. Cook, A. Abass and R. A. Collins, *Sens. Actuators B*, 1998, **49**(3), 235–239.
8 R. L. van Ewyk, A. V. Chadwick and J. D. Wright, *J. Chem. Soc., Faraday Trans. 1*, 1981, **77**, 73.
9 B. Bott and T. A. Jones, *Sens. Actuators*, 1984, **5**, 43.
10 M. J. Jory, P. S. Cann and J. R. Sambles, *J. Phys. D: Appl. Phys.*, 1994, **27**, 169.
11 A. Bradford, P. L. Drake, O. Worsfold, I. R. Peterson, D. J. Walton and G. J. Price, *Phys. Chem. Chem. Phys.*, 2001, **3**(9), 1750.
12 T. Richardson, V. C. Smith, R. A. W. Johnstone, A. J. F. N. Sobral and A. M. d'A Rocha-Gonsalves, *Thin Solid Films*, 1998, **327–329**, 315.
13 (*a*) C. M. Dooling, O. Worsfold, T. H. Richardson, R. Tregonning, M. O. Vysotsky, C. A. Hunter, K. Kato, K. Shinbo and F. Kaneko, *J. Mater. Chem.*, 2001, **11**, 392; (*b*) J. M. Pedrosa, C. M. Dooling, T. H. Richardson, R. K. Hyde, C. A. Hunter, M. T. Martín and L. Camacho, *Langmuir*, in the press.
14 C. H. Lee and J. S. Lindsey, *Tetrahedron*, 1994, **50**, 11427.
15 P. Fromherz, *Rev. Sci. Instrum.*, 1975, **46**, 1380.
16 S. Yu. Elovich and G. M. Zhabrova Zhur, *Fiz. Khim.*, 1939, **13**, 1761.
17 D. P. Arnold, D. Manno, G. Micocci, A. Serra, A. Tepore and L. Valli, *Langmuir*, 1997, **13**, 5951.
18 O. Worsfold, C. M. Dooling, T. H. Richardson, M. O. Vysotsky, R. Tregonning, C. A. Hunter and C. Malins, *J. Mater. Chem.*, 2001, **11**, 399.
19 O. Altin, O. Ozbelge and T. Dogu, *J. Colloid Interface Sci.*, 1998, **198**, 130.
20 I. Langmuir, *J. Am. Chem. Soc.*, 1918, **40**, 1361.
21 B. Chague, J. P. Germain, C. Maleysson and H. Robert, *Sens. Actuators*, 1985, **7**, 199; S. Goldberg, *Plant Soil*, 1997, **193**, 35.